ARMY RESEARCH LABORATORY

Detection of Naturally Occurring Gear and Bearing Faults in a Helicopter Drivetrain

by Kelsen E. LaBerge, Eric C. Ames, and Brian D. Dykas

ARL-TR-6795 **January 2014**

NOTICES

Disclaimers

The findings in this report are not to be construed as an official Department of the Army position unless so designated by other authorized documents.

Citation of manufacturer's or trade names does not constitute an official endorsement or approval of the use thereof.

Destroy this report when it is no longer needed. Do not return it to the originator.

Army Research Laboratory
Aberdeen Proving Ground, MD 21005-5066

ARL-TR-6795 **January 2014**

Detection of Naturally Occurring Gear and Bearing Faults in a Helicopter Drivetrain

Kelsen E. LaBerge and Brian D. Dykas
Vehicle Technology Directorate, ARL

Eric C. Ames
Aviation Applied Technology Directorate, AMRDEC

REPORT DOCUMENTATION PAGE	Form Approved OMB No. 0704-0188

1. REPORT DATE *(DD-MM-YYYY)*	2. REPORT TYPE	3. DATES COVERED (From - To)
January 2014	Final	September 2010–September 2012

4. TITLE AND SUBTITLE
Detection of Naturally Occurring Gear and Bearing Faults in a Helicopter Drivetrain

5a. CONTRACT NUMBER

5b. GRANT NUMBER

5c. PROGRAM ELEMENT NUMBER

6. AUTHOR(S)
Kelsen E. LaBerge, Eric C. Ames, and Brian D. Dykas

5d. PROJECT NUMBER

5e. TASK NUMBER

5f. WORK UNIT NUMBER

7. PERFORMING ORGANIZATION NAME(S) AND ADDRESS(ES)
U.S. Army Research Laboratory
ATTN: RDRL-VTP
Aberdeen Proving Ground, MD 21005-5066

8. PERFORMING ORGANIZATION REPORT NUMBER
ARL-TR-6795

9. SPONSORING/MONITORING AGENCY NAME(S) AND ADDRESS(ES)

10. SPONSOR/MONITOR'S ACRONYM(S)

11. SPONSOR/MONITOR'S REPORT NUMBER(S)

12. DISTRIBUTION/AVAILABILITY STATEMENT
Approved for public release; distribution is unlimited.

13. SUPPLEMENTARY NOTES

14. ABSTRACT

A high-load endurance test was performed on the tail drivetrain of an H-60 Blackhawk helicopter to determine the resistance to gear tooth fracture under power levels exceeding the maximum continuous rating. During posttest inspection, it was found that a tooth had broken off of the tail takeoff spiral bevel gear. In addition, a moderate spall was found on the outer race of the intermediate gearbox input gear shaft support bearing. There were no obvious indications of the gear tooth failure during the duration of the test, making the determination of the time of tooth fracture critical to understanding the resistance of the H-60 tail drivetrain to overloads. This report analyzes vibration data sampled periodically throughout the test to determine the initiation time of these two specific mechanical failures. Both faults occurred naturally in a system environment, making the dataset of particular interest. Several existing gear and bearing vibration analysis techniques were utilized. These methods clearly identified the time of initiation of both the spiral bevel gear tooth fracture and the bearing spall. The capability of the different analysis methods relative to predicting gear tooth crack and bearing spall initiation are compared.

15. SUBJECT TERMS
vibration analysis, fault diagnostics, gears, bearings, health monitoring, transmission

16. SECURITY CLASSIFICATION OF:			17. LIMITATION OF ABSTRACT	18. NUMBER OF PAGES	19a. NAME OF RESPONSIBLE PERSON
a. REPORT	b. ABSTRACT	c. THIS PAGE			Kelsen E. LaBerge
Unclassified	Unclassified	Unclassified	UU	26	19b. TELEPHONE NUMBER (*Include area code*) 216-433-2078

Contents

List of Figures

Acknowledgments

The authors would like to thank the Helicopter Drive System test team at the Naval Air Warfare Center. In particular, the authors would like to thank facility engineer Logan Haney for his help in providing research data, test notes, and facility data.

INTENTIONALLY LEFT BLANK.

1. Introduction

The H-60 helicopter is the workhorse utility helicopter for the U.S. Army. Specific maneuvers such as right sideward flight and aggressive left turns in a hover can produce high transient torques within the H-60 tail rotor drivetrain that are well above the maximum continuous power level at which the tail rotor drive system components are qualified. In an effort to examine the resilience of the tail drivetrain to such short-duration overload conditions, the Army's Aviation Applied Technology Directorate conducted high-load endurance testing on the H-60 tail drivetrain. This test was designed to assess the durability and fatigue capability of the tail drivetrain when subjected to short-to-moderate-duration transient loads exceeding 800 hp (595 kW).

The general layout of the H-60 tail drivetrain is shown in figure 1. It consists of five gearboxes: two input modules, the main rotor gearbox (MGB), the intermediate gearbox (IGB), and the tail rotor gearbox (TGB). After an initial reduction in the input modules, power is combined in the MGB by the left and right input pinions driving a large downward-facing spiral bevel gear. Bolted to the top face of the large spiral bevel gear is another spiral bevel gear referred to as the tail takeoff (TTO) gear (figure 2). From this gear, power is sent aft to the tail rotor through the TTO pinion. There is a single-stage spiral bevel reduction in the intermediate gearbox and a final spiral bevel reduction at the tail rotor gearbox.

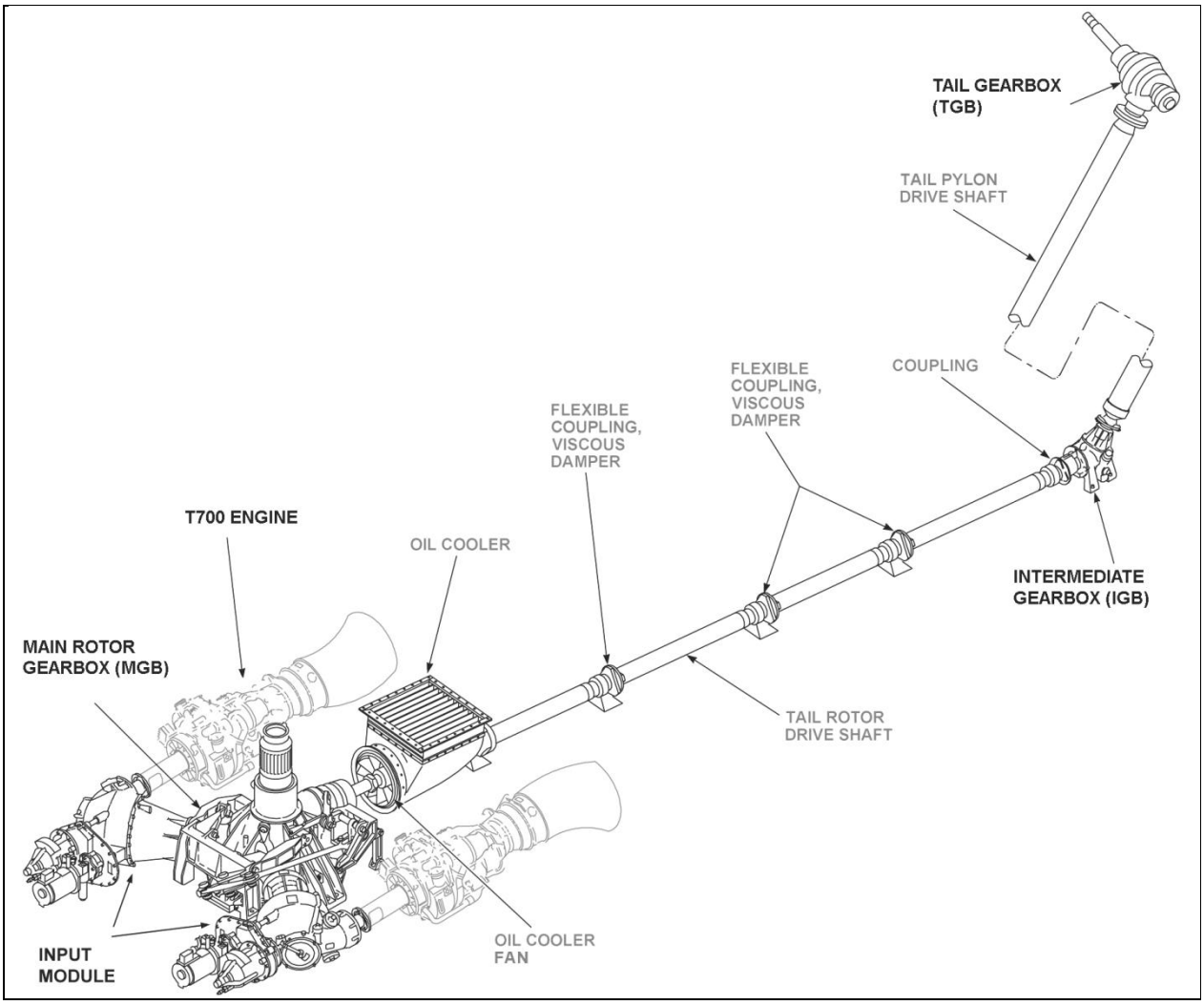

Figure 1. H-60 tail drivetrain schematic (*1*).

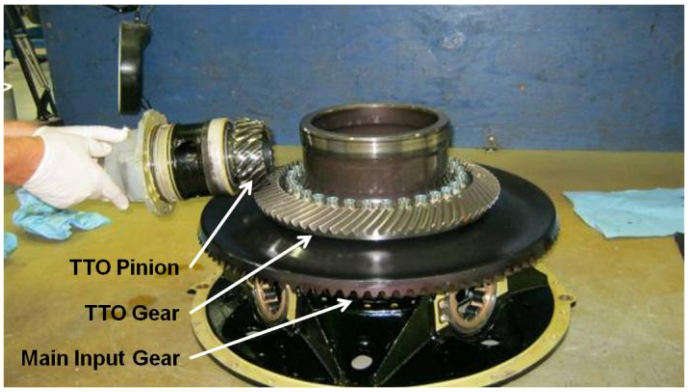

Figure 2. Disassembled input spiral bevel and TTO spiral bevel gears as well as the TTO pinion.

The tail drivetrain endurance test discussed here was performed at the Naval Air Warfare Center's Helicopter Drive System (HeDS) facility at Patuxent River, MD. The HeDS facility is a structural rig capable of physically supporting the H-60 MGB, input modules, IGB, and TGB. The layout of the rig is such that it closely simulates the H-60 drivetrain configuration. The HeDS facility uses two T700-GE-701C engines to drive the gearboxes during testing. Since this test focused on only the tail drive and minimal main rotor loads were applied, a single engine was used to provide torque to the tail drivetrain. Fractional load was applied to the main rotor output shaft by two water dynamometers mounted to the facility's speed-increasing gearbox. The tail rotor output shaft was loaded through a separate single-disk water dynamometer. The complete HeDS layout is shown in figure 3.

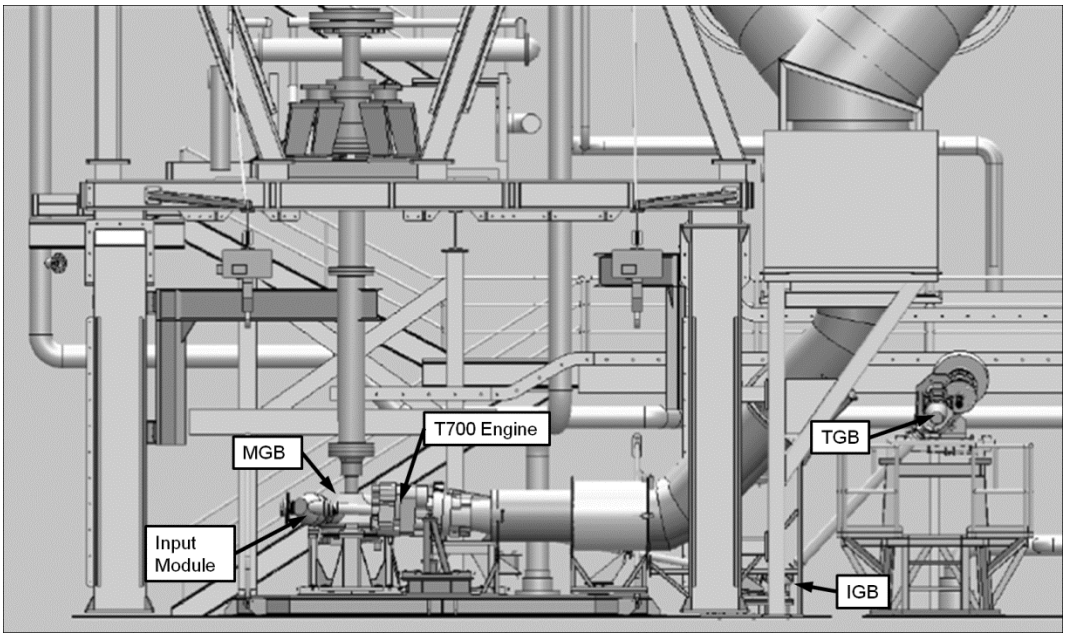

Figure 3. HeDS test facility layout.

Endurance testing was performed by cycling the power input to the tail drivetrain between 100 hp (75 kW) and 800 hp (595 kW) with a few shorter cycles of higher input power (upwards of 950 hp [700 kW]) toward the end of testing. The test was eventually halted due to increased vibrations in the IGB. The MGB, IGB, and TGB were then removed from the HeDS facility and sent for tear-down inspection. During tear-down, two components were found to have mechanical damage. The IGB was found to have a fatigue spall on the outer race of the inboard-input bearing, which caused the increased vibration that eventually suspended testing (figure 4). In addition, and perhaps more importantly, the TTO gear was found to have a complete tooth fracture (figure 5). There were no vibration, temperature, or particle indications noted in the MGB during in-service testing that signaled a problem.

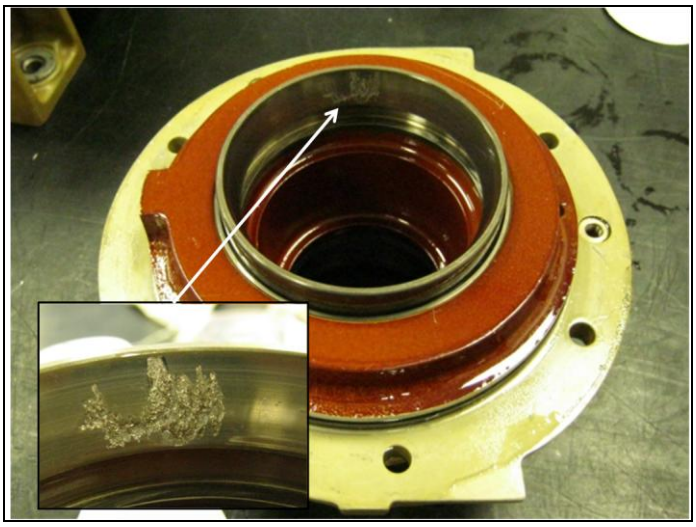

Figure 4. Spalled inboard-input IGB tapered roller bearing outer race.

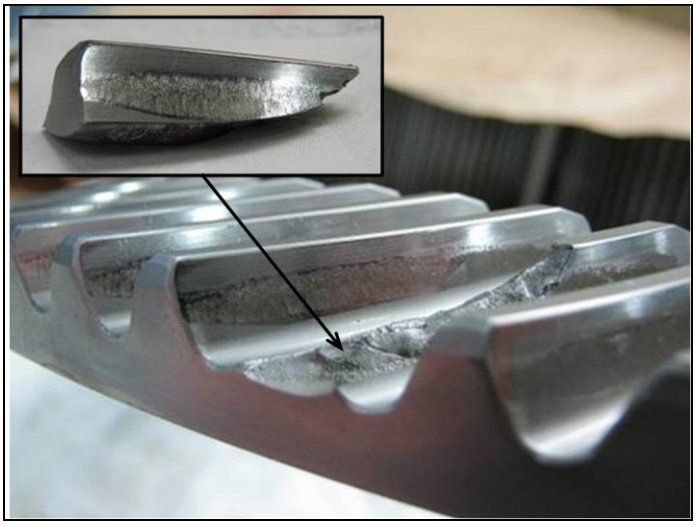

Figure 5. Fractured TTO gear tooth.

Many H-60 helicopters are equipped with the Goodrich Integrated Mechanical Diagnostics System (IMDS), an outline of which can be found in Dora et al. (*2*). This system is designed to process data from an array of sensors installed on the helicopter to determine the health of mechanical components. While the IMDS signal processing was not used during this test, data from the system's accelerometers was recorded during steady-state conditions at a sampling rate of 100 kHz.

Though accelerated by exposure to loading in excess of design loads, the gear and bearing faults discovered after testing were naturally occurring and unseeded. As such, the vibration data collected throughout the duration of the test provides a unique opportunity to compare the relative performance of mechanical diagnostic techniques on components that are located in a

helicopter drivetrain system. In addition, laboratory data testing is generally performed on a signal component or gearbox. While the vibration data obtained from this test is likely different from the data obtained with such a fault during flight, it does include the interaction between the different gearboxes and other dynamic components.

2. Background

2.1 Gear Diagnostics

When operating above rated power levels, the fatigue-induced cracking of gear teeth is a failure mode of particular concern. This failure mode can be difficult to diagnose, as cracks may not appreciably change the vibration signals until a crack has progressed through a large portion of a tooth. Fatigue cracks also typically do not produce debris in quantities that will trip chip detectors. As a result, this failure mode typically provides less warning and can have more catastrophic consequences than a contact fatigue fault. In contrast, contact fatigue-induced spallation initiates and propagates with some advance warning (via chip detector or increased vibration) initially benign consequences. Because of this, helicopter manufacturers typically design their gears to fail via contact fatigue before there is a danger of cracking. While gear tooth cracks are uncommon in helicopters, it is still desired to have the capability detect this type of damage with installed health and usage monitoring systems.

Over the past 30 years, there has been extensive study in the area of gear diagnostics, particular in the field of rotorcraft. The study in this field has been fueled by the fact that rotorcraft maintenance is cost and labor intensive. One general area of gear diagnostics involves monitoring gearboxes equipped with accelerometers. This data is generally averaged, filtered, and analyzed to put the health of a component into a single number or condition indicator (CI). This is often done using statistical algorithms in which the vibration signature of a gearbox is processed to detect deviations from the expected vibration signature. CIs can quantitatively describe the health of a gearbox without the need to examine the entire vibration signature qualitatively at each acquisition step. A review of many typical CIs can be found in Samuel and Pines (*3*), many of which were designed to be sensitive to a specific gear fault mode (e.g., wear and localized contact fatigue). Though several CIs were used in this particular analysis, only a few designed to be sensitive to localized tooth damage are discussed here.

All of the gear diagnostic techniques discussed herein require time-synchronous averaging of vibration signatures before statistical processing. Time synchronous averaging is performed by averaging vibration data from several rotations of the gear being analyzed, which removes signal components associated with noise and vibration of other components not synchronous with the gear of interest. With ideal regular gear vibration consisting of mainly meshing frequencies and harmonics, many gear CIs focus on information that falls outside of these frequencies. Therefore,

they are not computed directly from the signal average but rather from the difference signal, which is the averaged data with regular meshing frequencies, harmonics, and the shaft rotation frequency removed along with the associated first-order sidebands (*4*, *5*).

The gear CIs discussed in the following analysis include FM4, M8A, and NB4. The first two are calculated from statistics-based algorithms using the difference signal. FM4 is traditionally defined as the normalized kurtosis of the difference signal, or the fourth moment divided by the square of the variance (*4*), though several variants have been documented (*6*). Kurtosis is a statistical term that describes the general "spikiness" of a signal. Thus, a signal with a small number of high-amplitude peaks would have a large kurtosis. Given a difference signal composed of pure Gaussian noise, the FM4 CI would have a nominal value of 3. Equation 1 gives the formula for the FM4 CI, where d_i is the ith point in the difference signal, $\bar{d}$ is the mean of the difference signal, and N is the total number of points in the difference signal.

$$\mathrm{FM4}=\frac{N\sum_{i=1}^{N}\left(d_i-\bar{d}\right)^4}{\left[\sum_{i=1}^{N}\left(d_i-\bar{d}\right)^2\right]^2} \tag{1}$$

Similarly, the M8A CI is defined as the eighth moment over the variance to the fourth power as shown in equation 2. This CI was developed to be even more sensitive to localized damage than FM4; however, CIs highly sensitive to peaks in the difference signal are not always the best fault indicators as they can result in a higher incidence of false positives. Nominal conditions would result in a value of 105 for M8A (*7*).

$$\mathrm{M8A}=\frac{N^3\sum_{i=1}^{N}\left(d_i-\bar{d}\right)^8}{\left[\sum_{i=1}^{N}\left(d_i-\bar{d}\right)^2\right]^4} \tag{2}$$

McFadden demonstrated the usefulness of amplitude and phase demodulation in detecting fatigue cracks (*8*). The complex analytic signal is then computed by way of equation 3, where b is the filtered signal and H is the Hilbert transform. From here, the amplitude and phase of the complex analytic signal s provides the amplitude and phase modulation signals. The presence of a fatigue crack in a gear tooth will cause a lag in the phase and a change in the amplitude of the modulating signal (*8*).

$$s[n]=b[n]+iH\{b[n]\} \tag{3}$$

Though the phase and amplitude demodulation technique described by McFadden gives an indication of a fatigue crack in a gear, this requires the vibration at each acquisition point to be qualitatively examined. In the case of NB4, the averaged signal is bandpass-filtered around the primary meshing frequency, including all sidebands and excluding the actual mesh frequency. The amplitude modulating signal is then calculated as described. The NB4 metric builds on McFadden's concept by computing the quasi-normalized kurtosis from the resulting amplitude

modulating signal (*9*). This metric effectively builds on McFadden's method to generate a quantitative indication of gear health, and has been shown in previous studies to be effective at identifying tooth cracks (*10, 11*).

2.2 Bearing Diagnostics

The development of pits in bearing components is the failure mode of interest here due to the outer race pit discovered in the IGB input bearing. As rolling elements over-roll a flaw in a raceway, an impact is generated, which excites structural natural frequencies, similar to modal impact testing. These over-roll impacts occur at a specific interval according to the movement of the balls with respect to the flaw. Given the bearing geometry and rotational speed, the rate at which over-roll occurs can be determined. By assuming that there is no slip between the rolling elements and raceways, four different fault frequencies can be calculated: the ball pass frequency for the inner and outer races (referred to as BPFI and BPFO, respectively), and the ball spin frequency and cage rotation frequency (*12*). Actual fault frequencies may differ slightly depending on the amount of slip in the bearing.

In the presence of their respective bearing faults, these frequencies are not necessarily seen in the raw frequency spectrum because the over-roll behavior is actually a modulation. Demodulation is therefore used to extract the modulating function from the structural vibration content. The signal is first bandpass-filtered around structural natural frequencies. The amplitude modulating signal or envelope can then be computed using equation 3. As with gear diagnostics, there are many different methods available for bearing fault detection, not all of which use this method of demodulation. Since the resulting fault is already known to be in the outer race, the only two bearing CIs discussed here are the magnitude of the amplitude modulating signal at the BPFO and the root mean squared (RMS) of the amplitude modulating signal.

3. Experimental Setup

As stated in the introduction, the goal of this test was to assess the durability and fatigue capability of the H-60 tail drivetrain under short-duration loads up to 200% of the continuous operation design point. Before installation, the MGB, IGB and TGB were overhauled by a certified facility. Existing used gears with minimal run time were used in the TGB and IGB. The MGB was reassembled with a new TTO gear and pinion. Following overhaul, the gearboxes were returned to the HeDS facility and installed.

The endurance tests were performed by cyclically loading the tail drivetrain between 100 hp (75 kW) and 800 hp (595 kW) according to the drive cycle shown in figure 6a. Operating temperatures on the IGB began to increase starting around the 10th sequence-A load cycle. As the testing proceeded, the loading sequence was optimized around the thermal performance of

the IGB. The drive cycle was altered by removing intermediate steps, shortening the time spent at maximum loads and reducing the minimum load in order to allow the IGB more time to cool. As the test progressed, IGB vibration levels increased and the ability to dwell at 800 hp (595 kW) decreased.

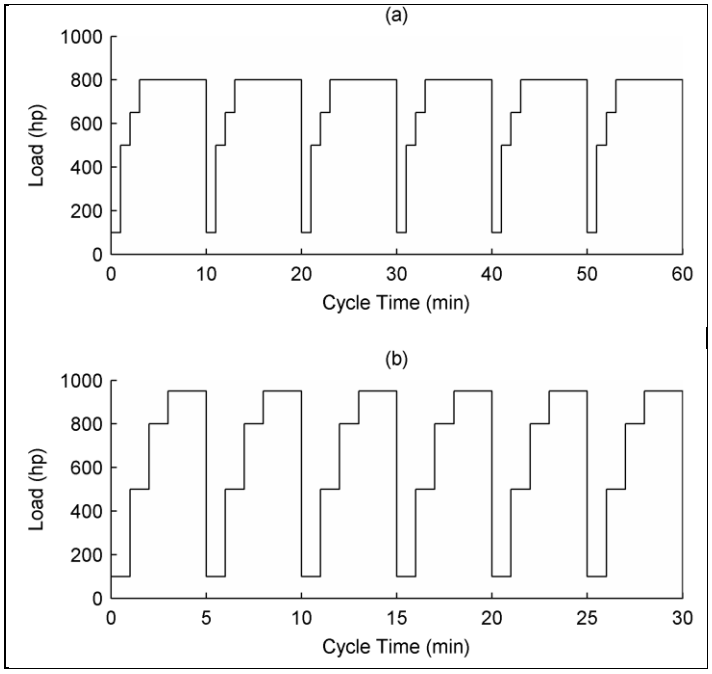

Figure 6. Load sequence plots for both sequence A (a) and B (b).

In an effort to acquire some data at higher loads, the drive cycle was changed to sequence B (figure 6b). During sequence B testing, approximately 60 min of run time was accumulated at power levels of approximately 950 hp (708 kW). Again, the drive cycle was optimized around the thermal performance of the IGB; however, testing was eventually stopped due to increased vibration in the IGB just prior to 28 h of run time.

Both facility and research data was acquired during testing. Facility data, including torque, speed, temperature, and vibration measurements, were acquired continuously throughout testing at 1Hz. Raw data was acquired from the Goodrich IMDS sensors at 100 kHz for 5-s durations only when steady-state conditions existed. The sensors installed on the MGB and IGB are shown in figure 7, circled in red. For the TTO gear failure analysis, data collected from the TTO radial accelerometer (mounted on the housing adjacent to the TTO pinion bearing) was used. This sensor was in the most direct force path to the TTO gear being analyzed. Similarly, the data used to determine the fault initiation time of the IGB bearing came from an accelerometer mounted in close proximity to the input bearing on the IGB.

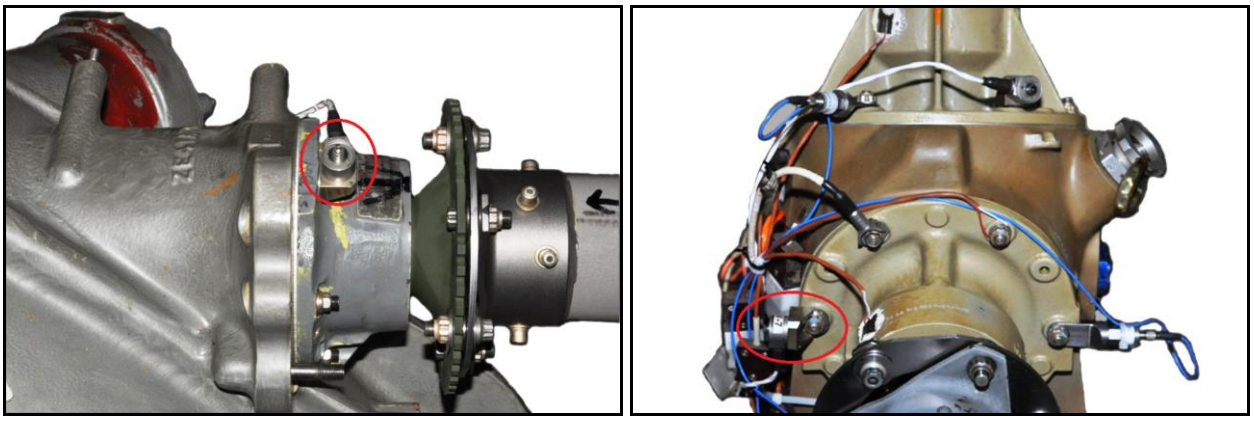

Figure 7. Instrumented MGB housing at the TTO (left) and IGB housing at the input (right).

4. Results

As discussed in the Introduction, the TTO gear is bolted to the input spiral bevel gear, each of which has a different number of gear teeth (75 and 100 teeth, respectively). Therefore, when time synchronous averaging (TSA) of the TTO radial accelerometer signal is performed with respect to the TTO gear rotation, the meshing frequencies of the input spiral bevel are still present. This can be seen in the frequency spectrum in figure 8, where the TTO meshing frequency harmonics appear at multiples of 75 shaft orders (N) and the input spiral bevel meshing harmonics appear at multiples of 100 shaft orders (M). Two analyses were performed for comparison. The first only removed the TTO gear meshing frequencies from the difference and residual signals, while the second was performed removing the input bevel mesh frequency harmonics in addition to the TTO gear meshing frequency harmonics. This resulted in an increased sensitivity of the CIs to the crack in the TTO gear.

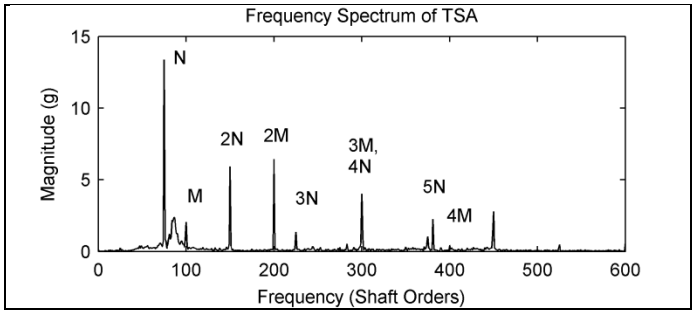

Figure 8. Frequency spectrum of TSA includes both the TTO gear-mesh harmonics (N) and the input spiral bevel-mesh harmonics (M) as calculated from the TTO radial accelerometer.

Figure 9 shows the CI progression during the last few hours of testing along with the applied load. (Continuous load data is estimated between hours 23 and 26 due to a computer power failure.) While several common CIs were calculated, for the sake of space only those discussed previously are presented here. These plots include the CI results obtained leaving the input bevel mesh frequency and harmonics intact beside the results obtained by removing them. In each CI presented, there is little or no change for the first 25 h of testing despite the maximum load increase to 950 hp (708 kW) shortly after hour 24. The first acquisition after hour 26 shows a sharp increase in these three CIs, indicating the presence of damage. These CIs continue to increase until approximately 26.5 h of testing, when they begin to fluctuate. Though the load affects the magnitude of the CIs, acquisitions at lower loads after expected crack initiation still demonstrate an increase over those taken before damage occurred.

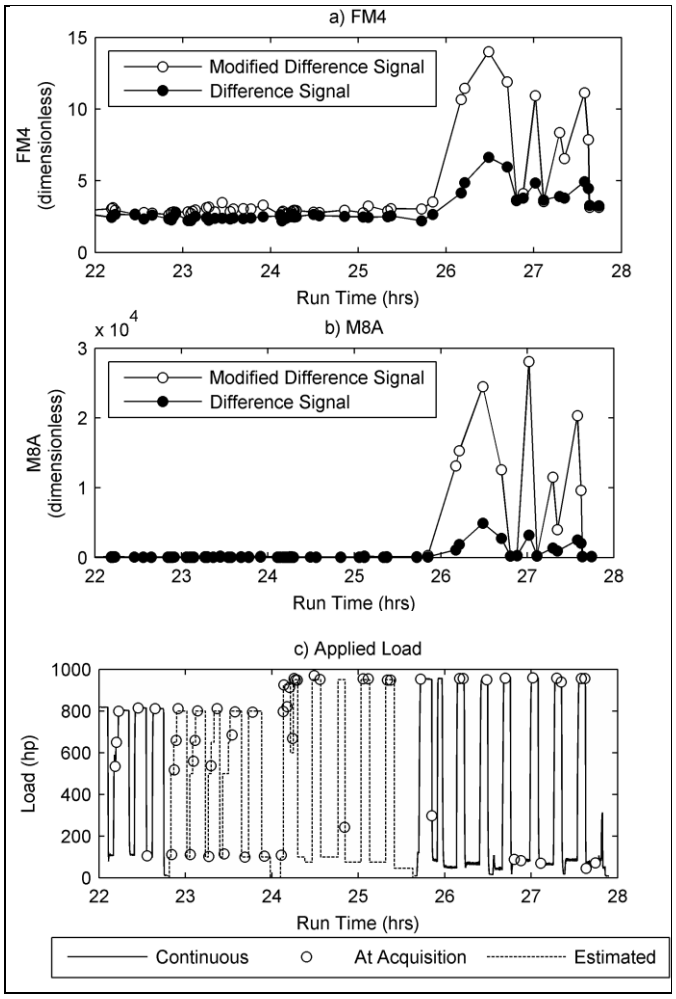

Figure 9. FM4 (a) and M8A (b) results during the final hours of testing. Results are plotted in line with the load (c).

The results for the NB4 CI are slightly different in nature because this CI does not use the difference signal. Figure 10 shows NB4 results during the final hours of testing. Similar to figure 9, the NB4 metric shows a sudden increase just before hour 26 of testing. NB4 continues to increase until approximately 26.7 h of testing, at which time it abruptly drops off. Unlike the other metrics, NB4 does not increase again for the remainder of the test. It is expected that the tooth failure occurred shortly after the peak in the NB4 metric around hour 26.7, causing the value to drop dramatically.

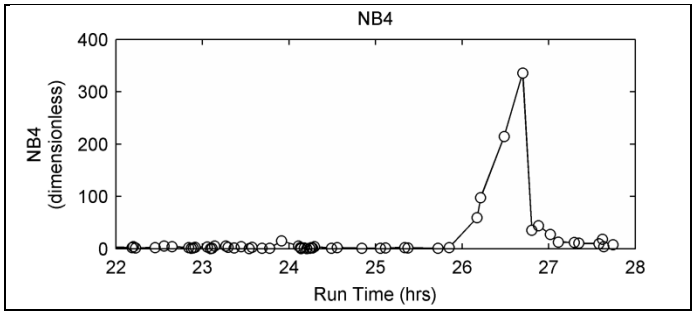

Figure 10. NB4 CI results for the final hours of testing.

Unaware of the tooth failure in the TTO gear, testing continued for a total run time of slightly less than 28 h when the test was suspended due to high vibration levels in the IGB. The tear down of the gearbox revealed an inboard-input bearing outer race spall shown in figure 4. Bearing CIs were computed from the raw data taken from a housing-mounted accelerometer installed in proximity of the IGB input bearing. Figure 11a shows the RMS of the amplitude-modulating signal calculated from the raw vibration signal bandpass filtered around structural frequencies (23–38 kHz). This pass-band should be identified via modal testing depending on the application. However, since the fault was already known in this case and the hardware was not accessible, a trial and error approach was taken to find the band that best captured the bearing fault.

Figure 11b shows the magnitude of the amplitude modulating signal at the BPFO (1047 Hz). Both the RMS of the modulating signal and the BPFO magnitude of the modulating signal give a good indication of the time of spall initiation. The magnitude of the BPFO shows the presence of a spall 21.5 h into testing, which is slightly earlier than the RMS. While the magnitude of the BPFO will indicate damage particularly in the outer race, the RMS will increase regardless of the bearing fault location, though with the modulating signal including information from all the possible bearing fault frequencies, it may be less sensitive to the presence of damage. The BPFO magnitude is more sensitive to torque fluctuations in the system, but even those data points taken at lower torques show an increase over prespall magnitudes for the BPFO. The RMS of the modulating signal shows less sensitivity to torque fluctuations.

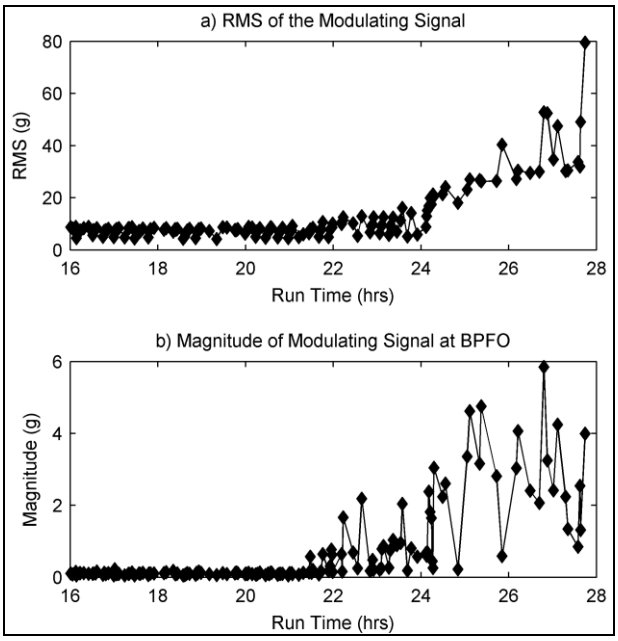

Figure 11. IGB bearing diagnostics where (a) shows the RMS of the modulating signal and (b) shows the magnitude of the modulating signal at the BPFO.

5. Conclusions

A tail rotor high-load endurance test was performed on an H-60 drive system at the HeDS facility located at the Naval Air Warfare Center in Patuxent River, MD. Posttest inspections revealed a spall on the IGB inboard-input bearing and a broken tooth on the TTO gear, the latter giving no indication of damage during testing. A gear and bearing posttest vibration analysis was performed. Analysis of the vibration from the TTO radial accelerometer determined the approximate time at which a TTO gear tooth crack initiated and progressed to tooth failure. CIs detected the crack sometime around hour 26 of run time, and failure was diagnosed after 26.7 h. While the gear CIs discussed gave an indication of damage shortly after 26 h, this should not be confused for the point of crack initiation, but rather the point at which the fault is detectable using these algorithms.

Also performed was an analysis of the vibration from the IGB inboard-input bearing, which contained a large spall in the outer race. Using the magnitude of the modulating signal at the BPFO, the spall is initially detected at around 21.5 h, though this CI was sensitive to the fluctuations in torque. The RMS of the modulating signal gave an indication of damage in hour 22, but was less sensitive to the applied torque. This is 4.5 h before the first detection of damage

in the TTO gear. This analysis shows that the tail drive of an H-60 is able to survive repeated short bursts of tail overloads up to 800 hp, with the weakest link being the inboard-input IGB bearing.

While the analyses discussed here clearly identify the presence of damage in the system, similar real-time analyses of rotorcraft field data is not as simple. The loads and acquisitions in this case were controlled by facility engineers. In contrast, the loads experienced by an actual aircraft are much less predictable, and steady-state conditions likely occur less often. Less-frequent acquisitions can decrease the amount of time damage is known prior to a potential failure. It is also important to consider the fact that the damaged components analyzed here were known prior to analysis, simplifying the process. Since each aircraft is subjected to different flight loads, additional components would need to be monitored to give a true picture of drive system health.

6. References

1. *U.S. Army, Aviation Unit and Intermediate Maintenance for Army Models UH-60M and HH-60M Helicopters;* TM 1-1520-280-23; Department of the Army: Washington, DC, 2007.
2. Dora, R.; Baker, T.; Hess, R. Application of the IMD HUMS to the UH-60A Blackhawk. Presented at the American Helicopter Society 58th Annual Forum, Montreal, Canada, 2002.
3. Samuel, P. D.; Pines, D. J. A Review of Vibration Based Techniques for Helicopter Transmission Diagnostics. *Journal of Sound and Vibration* **2005,** *282,* 475–508.
4. Stewart, R. M. *Some Useful Data Analysis Techniques for Gearbox Diagnostics;* UKMHM/R/10/77; Institute of Sound and Vibration Research, University of Southampton: UK, July 1977.
5. McFadden, P. D. *Examination of a Technique for the Early Detection of Failure in Gears by Signal Processing of the Time Domain Average of the Meshing Vibration;* AERO-PROP-TM-434; Department of Defence, Defence Science and Technology Organisation: Melbourne, Australia, April 1986.
6. Antolick, L. J.; Branning, J. S.; Wade, D. R.; Dempsey, P. J. Evaluation of Gear Condition Indicator Performance on Rotorcraft Fleet. Presented at the American Helicopter Society 66th Annual Forum, Phoenix, AZ, 2010.
7. Martin, H. R. Statistical Moment Analysis as a Means of Surface Damage Detection. Presented at the 7th International Modal Analysis Conference, Schenectady, NY, 1989.
8. McFadden, P. D. Detecting Fatigue Cracks in Gears by Amplitude and Phase Demodulation of the Meshing Vibration. *Journal of Vibration, Acoustics, Stress and Reliability in Design* **1986,** *108,* 165–170.
9. Zakrajsek, J. J.; Handschuh, R. F.; Decker, H. J. Application of Fault Detection Techniques to Spiral Bevel Gear Fatigue Data. Presented at the 48th Mechanical Failures Prevention Group Meeting, Wakefield, MA, 1994.
10. Zakrajsek J. J.; Lewicki, D. G. *Detecting Gear Tooth Fatigue Cracks in Advance of Complete Fracture;* NASA TM 107145, ARL-TR-970; U.S. Army Research Laboratory: Aberdeen Proving Ground, MD, April 1996.
11. Decker, H. J.; Lewicki, D. G. Spiral Bevel Pinion Crack Detection in a Helicopter Gearbox. Presented at the 59th Annual Forum and Technology Display, Phoenix, AZ, 2003.

12. Howard, I. *A Review of Rolling Element Bearing Vibration: Detection, Diagnosis, and Prognosis;* DSTO-RR-0013; Department of Defence, Defence Science and Technology Organisation, Aeronautical and Maritime Research Laboratories: Melbourne, Australia, 1994.

List of Symbols, Abbreviations, and Acronyms

BPFI	ball pass frequency inner
BPFO	ball pass frequency outer
CI	condition indicator
HeDS	Helicopter Drive System
IGB	intermediate gearbox
IMDS	Integrated Mechanical Diagnostics System
MGB	main rotor gearbox
TGB	tail rotor gearbox
TSA	time synchronous averaging
TTO	tail takeoff

NO. OF COPIES	ORGANIZATION
1 (PDF)	DEFENSE TECHNICAL INFORMATION CTR DTIC OCA
1 (PDF)	DIRECTOR US ARMY RESEARCH LAB IMAL HA
1 (PDF)	DIRECTOR US ARMY RESEARCH LAB RDRL CIO LL
1 (PDF)	GOVT PRINTG OFC A MALHOTRA
1 (PDF)	VEHICLE TECHNOLOGY RDRL VTP K LABERGE

INTENTIONALLY LEFT BLANK.